Seismic Assessment of a Cultural Heritage Minaret in Cairo

Hany M. Hassan, Mohamed A. Sayed, Marco Fasan, Fabio Romanelli, Claudio Amadio, Ayman Hamed, Mohamed ElGabry, and Islam Hamama

Abstract Dealing with cultural heritage is a sensitive process since each monument has its history, story, conditions, and scharacter. In this work, we assessed and evaluated the seismic vulnerability of a well-preserved cultural heritage structure that is the minaret of the Madrasa of the Princess Tatar al-Higaziya in Cairo. We selected the minaret site's input seismic source based on a physics-based ground motion simulation named multi-scenario seismic input (MCSI). This seismic source was used for the assessment of the dynamic behaviour of the minaret. A detailed numerical model of the minaret was developed in SAP2000. An initial bi-directional response spectrum analysis was performed on the minaret, considering the coefficient of subgrade reaction of soil. Both a record of the 1992 Cairo earthquake and synthetic seismograms were used. The calculations confirm no damage in the case of the 1992 earthquake while, in the worst-case scenario, the minaret could suffer significant tensile stresses that exceed the tensile strength of the limestone material. Results

H. M. Hassan (✉) · M. A. Sayed · M. ElGabry · I. Hamama
National Research Institute of Astronomy and Geophysics, Helwan 11421, Cairo, Egypt
e-mail: hany_hassan@nriag.sci.eg

M. A. Sayed
Department of Civil Engineering, University of Toronto, Toronto, Canada

M. Fasan · C. Amadio
Department of Engineering and Architecture, University of Trieste, Trieste, Italy

F. Romanelli
Department of Mathematics and Geosciences, University of Trieste, Trieste, Italy

H. M. Hassan · M. A. Sayed · M. Fasan · F. Romanelli · C. Amadio · A. Hamed · M. ElGabry · I. Hamama
Faculty of Petroleum and Mining Engineering, Suez University, Suez, Egypt

H. M. Hassan · A. Hamed · M. ElGabry
North Africa Group for Earthquakes and Tsunami Studies (NAGET), Net40/OEA ICTP, Trieste, Italy

I. Hamama
School of Systems Engineering, Kochi University of Technology, 185, Miyanokuchi, Tosayamada, Kami 782-8502, Kochi, Japan

denote enormous cracking and even crushing in the minaret body, particularly at the base and at a geometry transition zone right above the base. Furthermore, the tensile stresses' level predicts collapse or severe minaret damage under the C-MCSI-50% bidirectional response spectrum load. Results were confirmed by time-history analyses performed on the model. The results emphasize the importance of predicting the behaviour of heritage and historical structures against strong earthquakes, especially for those that share similar structural characteristics (e.g., height, construction time and materials) with our case study historical structure.

Keywords Seismic assessment · Cultural heritage minaret · Scenario based approach · Historical Cairo · Seismic input · Dynamical behaviour analysis

1 Introduction

Egypt is located at the conjunction of the Mediterranean basin, Africa, and Asia's continents. It has been known for its history and geography. Egypt has a multicultural heritage (e.g., Ancient Egypt, Coptic, and Islamic monuments) known for its diversity and richness. This heritage, a symbol of identity and an essential element of our memory, holds our shared principles and values and must be transferred to future generations. Cultural heritage is a unique wealth, requiring particular attention such as security, management, restoration, and preservation from all kinds of impacts brought by natural and human activities. Conservation of cultural heritage involves protection and restoration using intervention strategies that effectively maintain a particular property in a condition close to the original one and for as long as possible.

Egypt is considered a country of low to moderate seismicity. The earthquake record infers that inland earthquakes of moderate strength can substantially damage standard and cultural heritage structures and buildings. During the 1992 Cairo earthquake of moment magnitude M_w 5.9, about 212 of 560 monuments in Cairo were reportedly damaged (Sykora et al. 1993). Although the earthquake was of intermediate magnitude, a maximum intensity of VIII on the Modified Mercalli Intensity (MMI) scale was reported in Cairo; while the maximum observed intensity in the historic Cairo area was VII (Sykora et al. 1993). Several seismic hazard assessment studies and reviews have been conducted on Egypt (e.g., Sawires et al. 2016, Hassan et al. 2017b, Gorshkov et al. 2019, Hassan et al. 2017a, ElGabry and Hassan 2021). In this paper, we refer to the results provided by Hassan et al. (2020), where the seismic input in Cairo was computed through physics-based ground motion simulations.

The process of finding and selecting a proper mitigation strategy against seismic action for cultural heritage buildings and structures is based on two factors: the accurate evaluation and estimation of the expected ground motion at the site of interest and understanding the performance of such buildings and structures during the earthquake shaking. The performance status and protection objectives developed for modern conventional (non-heritage) buildings are not directly applicable to heritage buildings since they do not address and share cultural concerns and often

different construction techniques. In fact, in the preservation of historical monuments against seismic shaking, it is well known that each building has its characteristics (e.g., structure type, age, construction materials, state of preservation, site conditions, expected ground motion level, and surroundings). Therefore, specific requirements and intervention strategies are required based on a rigorous and detailed evaluation of the factors mentioned above.

Historic Cairo is a UNESCO World CulturalCentre (WHC) site with its famous mosques, madrasas, hammams, and fountains. Although these buildings were built in periods that date back to more than ten centuries, many have survived earthquake events with no or minor damage; others have suffered severe or complete damage. This study presents an assessment of the seismic vulnerability of a well-preserved cultural heritage structure, the minaret of the Madrasa of the Princess Tatar al-Higaziya in the historic Cairo area, hereafter referred to as the minaret. The study's peculiarity is the use of site-specific synthetic accelerograms to represent the seismic demand at the site of interest adequately. These accelerograms are used for an assessment of the minaret's dynamic behaviour, obtained by joining seismological and structural aspects to understand this monument's performance under earthquake loading. This study may contribute to the understanding of the seismic conservation criteria for cultural heritage sites in Egypt.

The results of this work could be necessary for the seismic risk reduction of heritage structures, particularly for those constructed during the same time and having similar structural systems and components. The research findings encourage detecting proper mitigation measures for the minaret and are a step towards a comprehensivemanagementstrategy for this historic structure.

2 Structural Elements of the Madrasa

The Madrasa (meaning a school in Arabic) of princess Tatar al-Higaziyawas constructed in two stages. First, the mausoleum was built in 1348 as an extension to princess Tatar's house, then after thirteen years, the palace and the mausoleum were converted into the Madrasa (Williams 2008). The Madrasa complex consists of the mausoleum, a minaret, and an ablutions court. It is one of few schools endowed by a woman in Cairo. The school was built and endowed to educate orphan children, raise the daily prayers, and serve as a public library. A clear sketch of the school layout, a three-dimensional view, and a recent photo of the minaret are shown in Fig. 1.

The school has been restored several times and more recently by the Egyptian government and the German Cultural Centre in 1980–1982 (Mayer and Speiser 2007). The minaret is one of the most significant school elements, consisting of a 24.16 m vertical shaft above the ground level, and it lacks an upper cap or mabkhara (Mayer and Speiser 2007). The minaret's ground plan is squared, with a width of 3.45 m up to a height of 11 m. There is a transition above the base to an octagonal plan, which is further emphasized using bevelled corners. This minaret has been thoroughly studied after the 1992 Cairo earthquake to inspect the level of damage

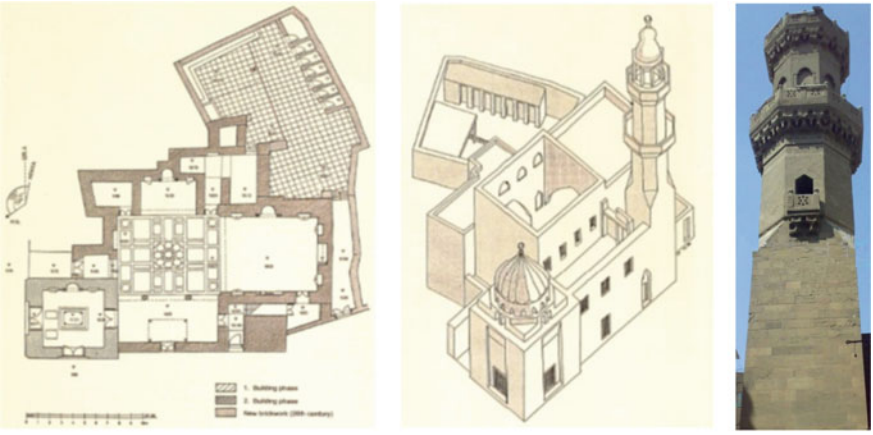

(a) (b) (c)

(d)

Fig. 1 Madrasa of the princess Tatar al-Higaziya: **a** layout, the filled brown square indicates the position of the minaret; **b** three-dimensional view; **c** recent photo of the minaret by the first author on 28/09/2017 taken from south west direction; **d** Location map of the Madrasa (site), subsurface profiles and earthquake scenarios based on which the MCSI was computed

that occurred to the minaret surviving the earthquake. The minaret's performance under earthquake loading was examined, but important seismological and other input parameters lacked in the studies. In modelling, a simplified shaft model that ignores some critical structural elements without justification was considered.

Additionally, the excitation records used in the study were simply the elastic response spectra of the 475-year return period of the Egyptian Building code, which is not logical since the building age is already beyond that period. The UNESCO project framework conducted the study to restore historic Cairo (Imam 2001). The incomplete assessment of the minaret's seismic performance motivated this study to reevaluatethe minaret's dynamic response using historical and recent seismic input and detailed numerical modelling techniques.

Several previous studies have introduced the numerical modelling and dynamic analysis of historical minarets under earthquake loading. For example, El-Attar et al. (2005) proposed a seismic protection technique for a historic limestone masonry minaret built between 1348 and 1960 AD in historic Cairo. In their study, the minaret was built one year after the minaret was reviewed in this study, with the same construction techniques and limestone material properties. Moreover, they considered a linear elastic finite element model in SAP2000 for the minaret, while the modal analysis results were evaluated and compared with ambient vibration test results. Sezen et al. (2008) have investigated the dynamic analysis and assessment of a reinforced concrete cylinder minaret constructed in Turkey. They developed four finite element models in SAP2000 representing the same minaret while ignoring various structural components in each model, such as openings, balconies, and interior spiral stairs, to arise a simplified numerical modelling approach for similar cylindrical minarets. They concluded that ignoring the spiral stairs' modelling influenced the modal analysis and modal participation factor, reducing the minaret's stresses. In the view of the studies mentioned above, we constructed our model considering all openings, balconies, and geometrical transitions while ignoring the spiral stairs for a conservative estimation.

3 Selection of Response Spectra and Time Histories

The multi-scenario physics-based seismic input (hereafter abbreviated as MCSI) provided in Hassan et al. (2020) represents a useful and conservative response spectrum analysis tool. Hassan et al (2017b) have provided a set of seismic hazard maps computed within the framework of NDSHA procedure at a national scale that may effectively accommodate any reliable new information to adequately compute the ground shaking scenarios maps. At local scale, further investigations can be performed within NDSHA taking into account the source effects and local soil conditions (i.e., surface and subsurface topography, resonance, water content, wave conversions, and geometry and heterogeneity of the sedimentary layers). In the work of Hassan et al. (2020), the map of the seismic sources that contribute to peak ground motion values at the historic Cairo area obtained using the NDSHA approach (Hassan et al. 2017a, b) is used for the definition of the earthquake scenarios that could affect a given site; this is needed to be considered for the detailed SSA studies in order to investigate the modification in the ground motion parameters due to the source, propagation medium, and the possible local site conditions and to obtain the MCSI.

Three earthquake scenarios have been found to be of magnitude 5.9–7.0 Mw earthquakes at a distance between 10 and 25 km, north and west of the site of interest. The selected scenarios comprise two historical events (i.e., 857 and 950 both of them have intensity MMI = IX) and one instrumental (i.e., 1992 of MMI = VIII). 1D laterally non varying structural model was considered to compute the seismic input at the bedrock level. The computed seismic input was feed up into 2D laterally varying model that represent the subsurface condition (Fig. 1d).

MCSI is being recommended for the seismic design of new structures, although it might be less suited to selecting accelerograms that can be used for dynamic analysis of existing structures. Since MCSI is based on the computation of synthetic accelerograms when running time history analyses, a fast and effective accelerogram selection method could be utilized. The number of the selected accelerograms depends on the number of rupture realizations, rupture styles, and directivity angles considered for every simulated scenarios that contributes to the MCSI spectra computed for the site as shown in Fig. 1d (Hassan et al. 2020). However, this can become impractical due to the enormous amount of time histories (on the order of thousands of simulated accelerograms), requiring long computational times, significant analysis efforts and massive machine power.

Figure 2a, b shows the seismic input computed at bedrock (MCSIBD) and considering the site-specific soil stratigraphy ($MCSI_{SS}$) (values of the 50th, 84th and 95th percentiles) compared with the elastic spectra from the Egyptian building code (ECP-201 2011) (Type 1 is devoted for the whole country and Type 2 for the coastal zone along the Mediterranean) for different return periods (recurrence intervals) and different site conditions, i.e., bedrock and soil site of type B (soil with shear wave velocity of 360–800 m/s) according to the soil classification provided by the Egyptian building code (ECP-201 2011). The peak ground acceleration for two return periods (i.e., 475 and 2475) was used to scale the elastic response spectra defined by the Egyptian building code, the PGA value for 475-year spectra (PGA = 0.15 g) is adopted from the Egyptian building code (ECP-201 2011), while the PGA for 2475 return period (PGA = 0.25 g) is taken from a recent study done by Gaber et al. (2018).

Since we are dealing with an already existing structure and our aim is evaluating its dynamic behaviour through time history analyses, there is a need to find an approach for the proper selection of time histories. As suggested by Fasan (2017), when using a multi-scenario physics-based seismic hazard assessment, an approach to select a restricted number of accelerograms could be to limit our selection to the earthquake scenario that controls the seismic hazard at the structural vibrational periods of interest. This seismic input at the fundamental period of the building of interest is defined as a "Conditional" (C-MCSI), as proposed by Fasan (2017). The concept is similar to what is called Conditional Mean Spectrum (CMS), proposed by Baker and Cornell in (2006) as a more realistic alternative to the UHS (Baker 2011; Baker and Cornell 2006).

C-MCSI response spectrum can be defined by considering the most hazardous source's spectral accelerations at the period of interest, contrasting with MCSI that should consider all possible scenarios. In our case, the minaret's fundamental period

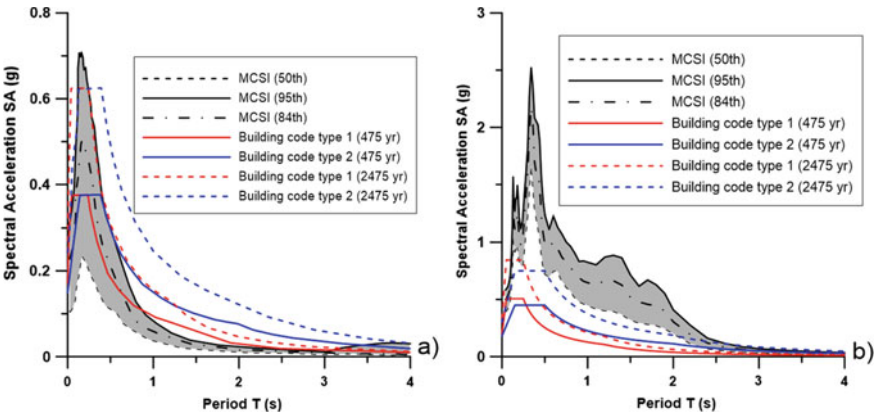

Fig. 2 **a** $MCSI_{BD}$ for the values of the 50, 84 and 95th percentiles, compared to the building code (Type 1 and Type 2) for two different return periods (475 and 2475 years). **b** $MCSI_{ss}$ for the values of the 50, 84 and 95th percentiles, compared to the building code (Type 1 and Type 2) of different return periods (475 and 2475 years) and the adopting recommended site coefficient. Shaded areas represent the range between 50 and 95th percentiles

is 0.5 s, as inferred from the noise measurements described in the next section. Figure 3 shows the C-MCSI for a period of 0.43 s, and the MCSI computed for the minaret site, which is set equal to the value of the 50th percentile and compared to the building code (Type 1 and Type 2) after considering site-effects.Fig. 4 shows the 50th C-MCSI and 1992 Cairo earthquake response spectra computed at 5% damping at the minaret site. They will be adopted to analyze the seismic performance for the minaret structure in the next section. C-MCSI response spectrum is calculated by selecting only the simulations from the scenario with a median spectral acceleration corresponding to the 50th percentile at the period of interest and then choosing the median values of these simulations at each period. The C-MCSI spectra account for the most dangerous scenario's spectral shape at the period of interest (Fasan 2017). Figure 3 indicates that both 50th C-MCSI and $MCSI_{SS}$ spectra vastly exceed the elastic response spectra defined by the building code (Type 1 and 2) for return periods of 475 and 2475 years.

Adopting this approach, the selection of accelerograms for the structural analysis becomes immediate since it merely retrieves the simulations used to define the C-MCSI. A subset of C-MCSI spectrum compatible accelerograms (e.g., seven, as suggested by building codes) are selected to conduct time history analysis. In our case, we have chosen seven simulations with two horizontal components, i.e., 14 accelerograms. The seven selected C-MCSI time histories in EW and NS directions at the minaret site and their corresponding response spectra of the ground motion components are plotted in Fig. 5. Once the accelerograms are selected, they can be considered a seismic input for the minaret's engineering model. Moreover, it is worth to mention that the seismic behaviour of a masonry structure is strongly influenced

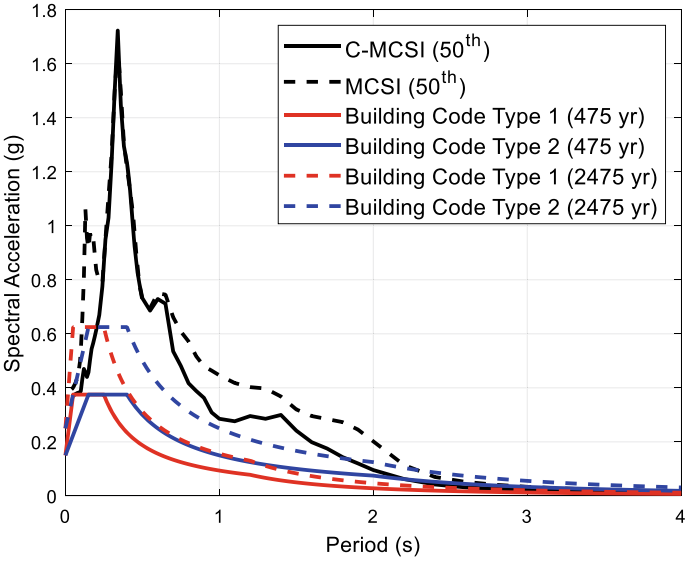

Fig. 3 C-MCSI and MCSI of 50th percentile response spectra compared with Type 1 and Type 2 Building Code with site-effect consideration at 5% damping

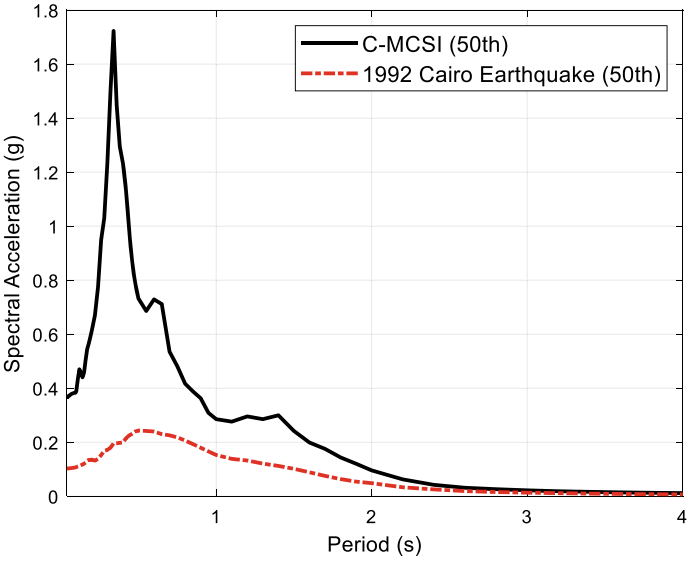

Fig. 4 C-MCSI and 1992 Cairo earthquake response spectra at 5% damping

by axial stresses which can be strongly modified by the vertical component of the seismic load, especially if they are located near the fault (Rinaldin et al. 2019).

4 Minaret Modelling

The minaret consists of a vertical shaft of a total height of 24.16 m. The minaret base is squared, after which there is a transition to an octagonal plan, further emphasized by bevelled corners. There are two tiers of balconies with stone parapets, accessed by an internal stone spiral staircase. A cylindrical shaft containing the inner spiral staircase extends from 7.2 m above the ground to the minaret's crest. The minaret dimensions and geometry is illustrated in Fig. 6.

A previous study performed by Imam (2001) on the structural condition of the Madrasa and its buildings was conducted in 2001 as part of the national historic Cairo project. The study affirmed that the minaret is structurally separated from the Madrasa with a vertical gap or separator. Moreover, five stone cone samples from three different parts of the Madrasa were extracted by (Imam 2001) to assign the different values of the limestone's mechanical properties used in construction. The report found that the un-cracked stone samples have a specific weight of 2.0 Mg/m^3, compressive strength of 27.5 MPa, a tensile strength of 5.4 MPa, and Young's Modulus of 25.5 GPa.

The minaretwas visually and physically inspected to investigate cracking and construction materials condition. Correspondingly, ambient vibration measurements by deploying seismic instruments at different locations inside the minaret body were conducted. The ambient vibration was used to evaluate the minaret's modal frequencies of the generated finite element model. After precise inspection, no visible cracks were detected in the minaret body, around the different openings, or near the joints. Therefore, un-cracked limestone material properties are considered in the minaret modelling with values stated previously.

4.1 Ambient Vibrations Analysis

The ambient vibration measurements were significant for the calibration of the dynamic behaviour of the minaret numerical model. Four tri-axial accelerometers with a range of ± 4 g were installed at different heights on the minaret to record the minaret's ambient vibration response. The sensors' locations are as follows: sensor (U1) was installed at the top balcony, and sensor U2 at ground level, sensors U3 and U4 were placed at the first balcony and the entrance, respectively. The sensors' locations are illustrated in Fig. 6. The McSIES-MT NEO (OYO Corporation) data acquisition instrument for microtremors measurement and vibration monitoring was used for the ambient vibration response analysis.

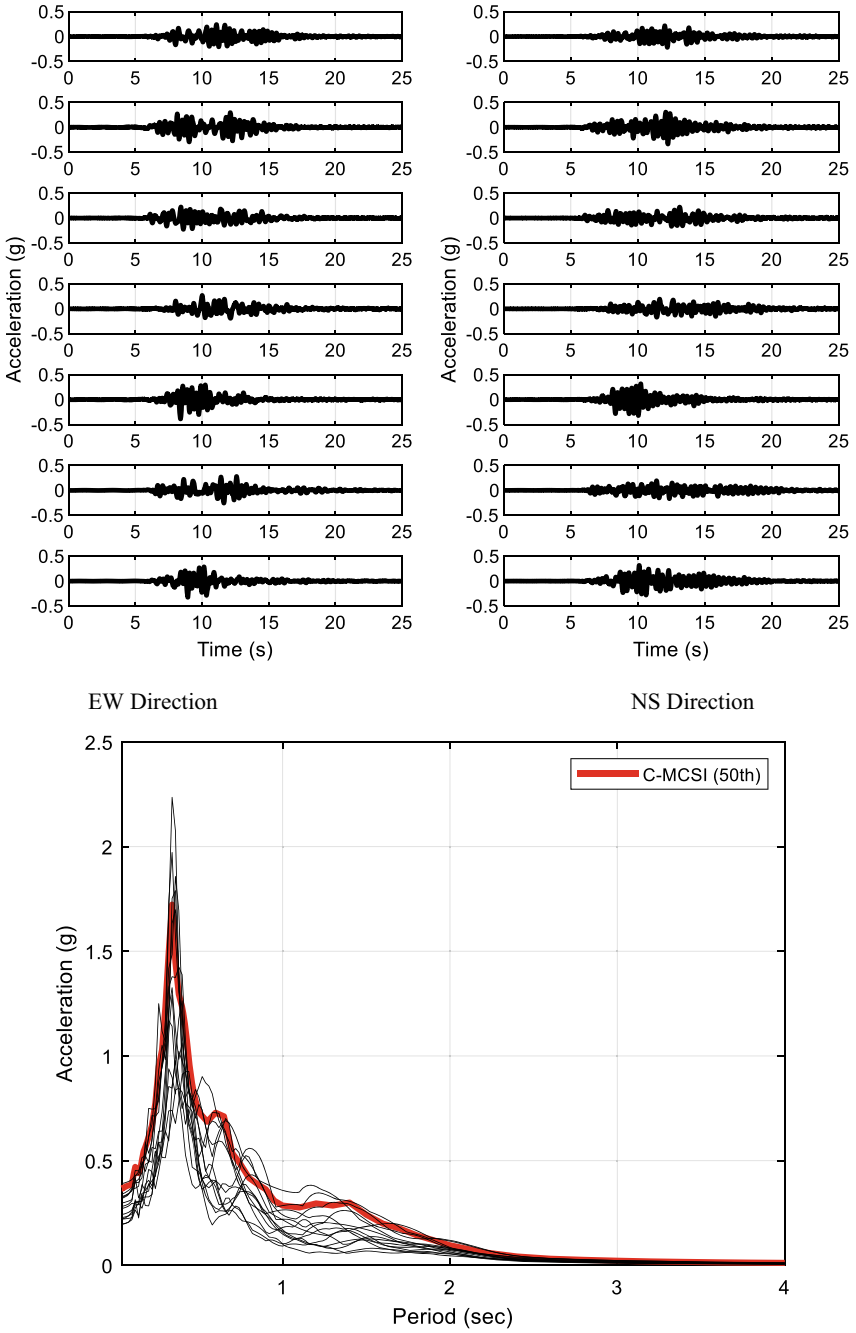

Fig. 5 Seven selected (on the median) C-MCSI time histories in EW and NS directions at the site of the minaret (top panel) and their corresponding response spectra withthe50th C-MCSI at 5% damping (bottom panel)

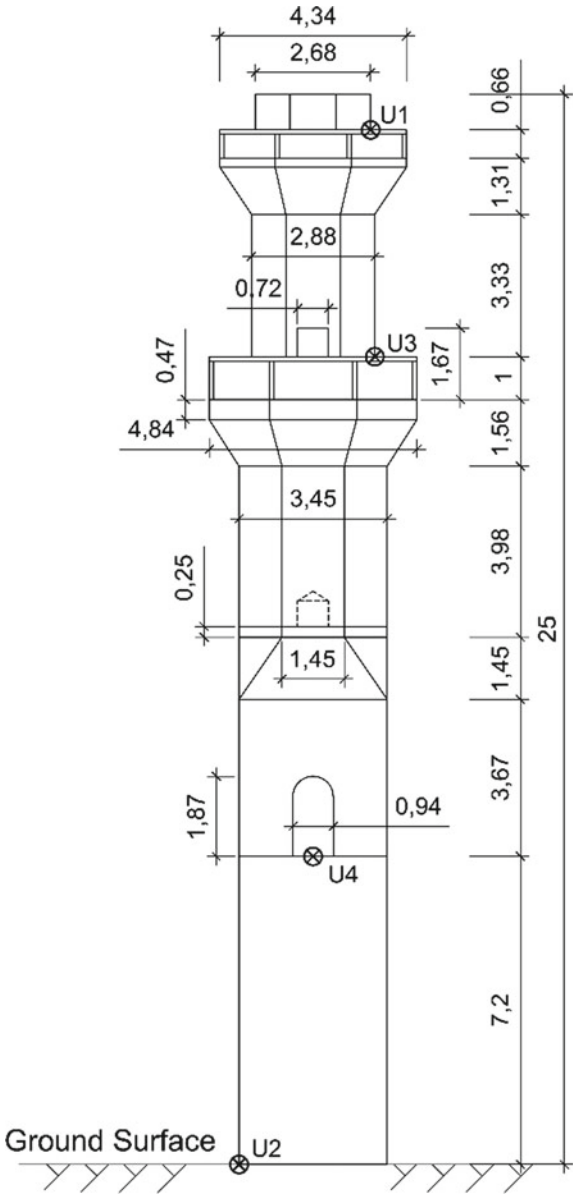

Fig. 6 Minaret geometry and instrumentation locations (all dimensions are in m). Instrument U1 installed at the top balcony; U2 at the ground surface; U3 at the lower balcony; U4 at the main entrance

The ambient vibration recording lasted for 60 min, with a recording sample frequency of 100 Hz. The measurements were recorded on a calm day with no moderate winds to eliminate weather effects on the ambient vibrations. It is also worth noting that the minaret is surrounded by taller buildings from all directions, reducing any wind effect on the minaret's ambient vibration. Post-processing of

the acceleration measurements with baseline correction and high-pass filter hasbeen considered. A fourth-order Butterworth high-pass filter was applied, and a corner frequency of 0.2 Hz for the selected filter is calculated as (Sayed et al. 2015):

$$f_c = \frac{1}{T\left[\frac{H_0}{1-H_0^2}\right]^{\frac{1}{2n}}} \tag{1}$$

where, f_c is the corner frequency, n is the high-pass filter order, T is the acceleration recording time, and H_0 is the filter amplitude threshold and selected as 0.02. The waveforms and power spectra at the top balcony (U1) and the lower balcony (U3) are depicted in Figs. 7, 8, 9 and 10.

Figure 7 and 9 illustrate the filtered recorded noise time history of the measurement points at the top and bottom balcony, respectively. Figures 8 and 10 show the power spectrum of the measurement points at the top and bottom balconies. The results show that the observed natural frequency of the minaret is about 2 Hz. Post-processing the different minaret measurement points such as U4confirms that the minaret's fundamental period is approximately 0.5 s. The ambient vibration results are correlated with the finite element model results in the following section.

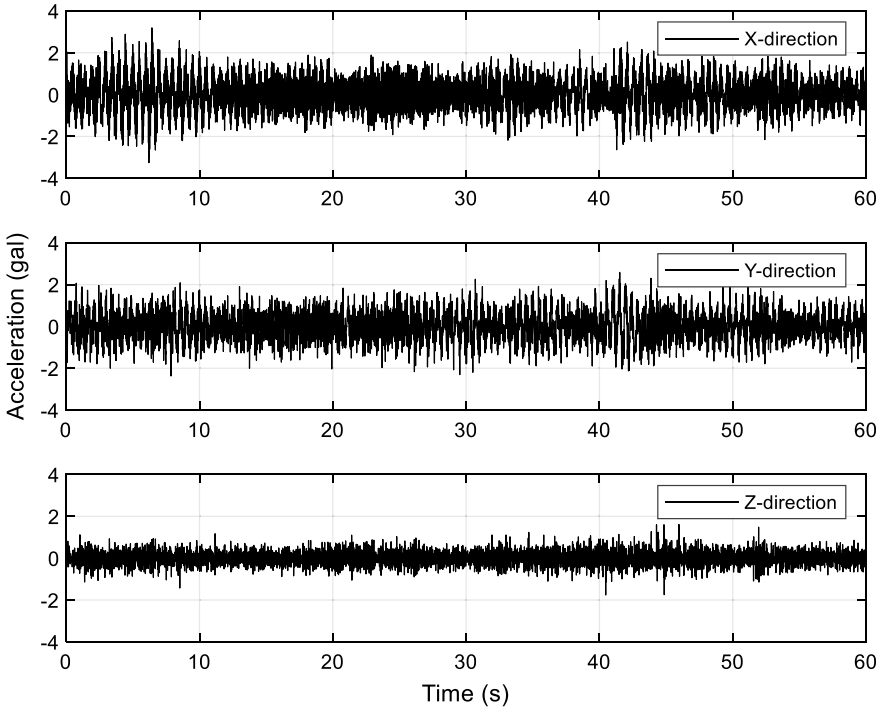

Fig. 7 Ambient noise time series in three directions at the top balcony (U1)

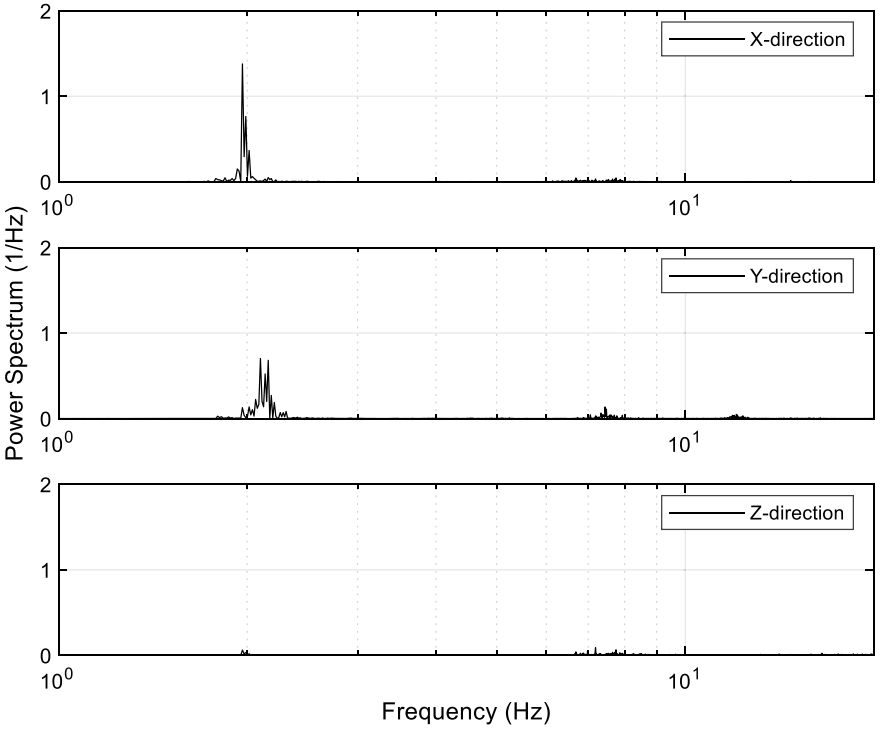

Fig. 8 Power spectra of the time histories in three directions at the top balcony (U1)

4.2 Numerical Model

The finite element (FE) numerical model of the minaret was developed in SAP2000. A linear elastic analysis was conducted for the minaret. The minaret's linear elastic model is a simplification, but it is coherent with preliminary assessments. Limestone minarets show limited dissipation capacity because limestone is typically a brittle material and that minarets are pendulum-like structures. Hence, a brittle failure without a plastic phase is reasonably expected to occur.

Moreover, no cracks were observed during the minaret inspection, suggesting a linear behaviour during the 1992 earthquake. The minaret base and shaft are modelled using eight-node solid elements, while the balcony posts are modelled as frame elements with a squared cross-section of 0.13 $\times$ 0.13 m. The balcony walls are modelled as shell elements with a thickness of 0.13 m. All the cross-sectional variations and openings in the minaret were accurately simulated in the numerical model. The spiral staircase was not modelled in this study for conservative modelling since ignoring modelling the spiral stairs insignificantly influenced the modal analysis and reduced the stresses (Sezen et al. 2008). Mesh sensitivity analysis is conducted to the minaret to produce a modal analysis close to the ambient vibration analysis.

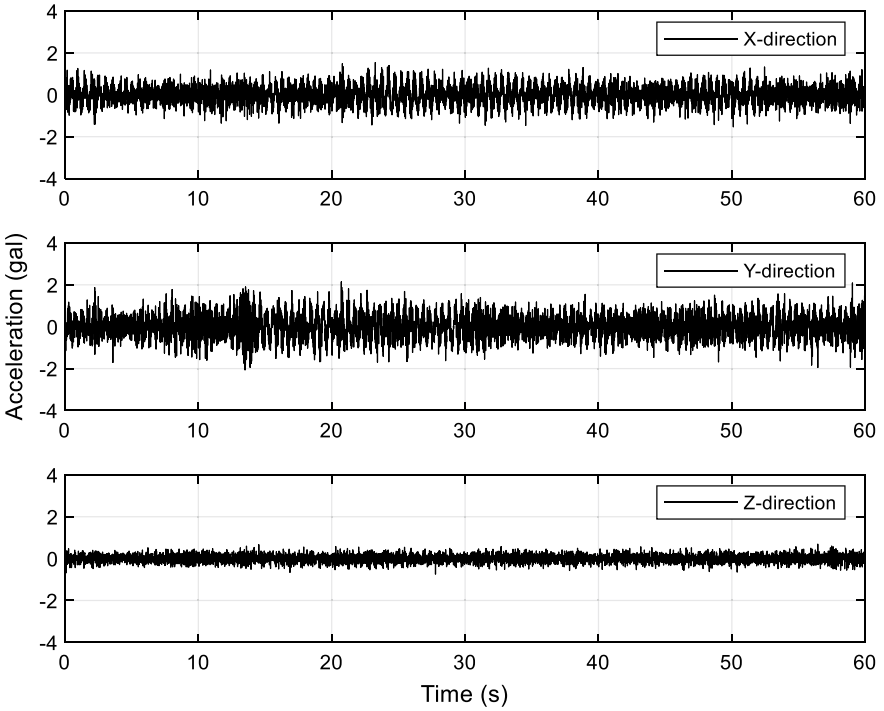

Fig. 9 Ambient noise time series in three directions at the first balcony (U3)

Following the minaret model discretization, the finite element model consists of 80,849 nodes, 64,355 solid elements, 16 frame elements, and 16 area elements. The total weight of the minaret is calculated as 4412.90 kN.

The soil beneath the minaret base is modelled as linear springs with a specified modulus of subgrade reaction. The soil modulus subgrade reaction was calculated using (Vesic 1961) as:

$$K_s = \frac{0.65E_s}{B\left(1-\upsilon_s^2\right)}\sqrt[12]{\frac{E_s B^4}{E_f I_f}} \tag{2}$$

where, K_s is the soil modulus subgrade reaction, E_s is the soil Young's modulus, B is the foundation width, υ_s is soil Poisson ratio, E_f and I_f are Young modulus and moment of inertia of the foundation, respectively. The soil properties beneath the minaret foundation are extracted from (Toni 2012) with a mass density of 1.5 Mg/m^3, shear wave velocity of 180 m/s, Poisson ratio of 0.30, and calculated soil Young modulus of 74.77 MPa. Moreover, the properties of the minaret foundation are considered as B of 3.45 m, E_f of 25.49 GPa and I_f of 11.80 m^4. The calculated soil modulus subgrade reaction is 11.71 N/mm^3. The modal analysis results and the comparison between the ambient vibration results, and the numerical model with

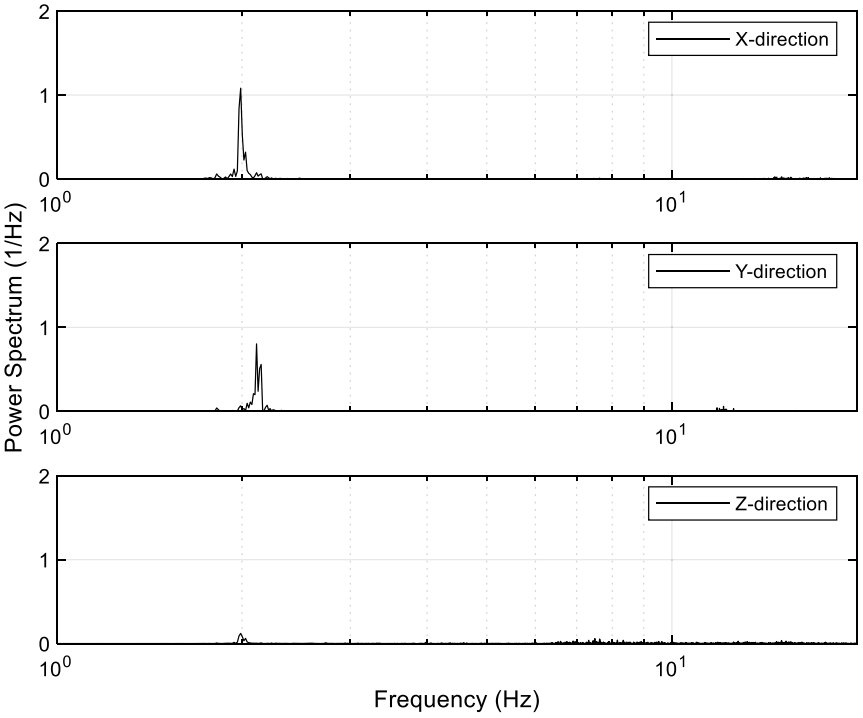

Fig. 10 Power spectra of the time histories in three directions at the first balcony (U3)

a modulus subgrade reaction, are given in Table 1. For comparison, the minaret's modal analysis with considering a fixed base condition is shown in Table 1. The difference between the period obtained from the noise measurements and the FE model is about 12%. The discrepancy could be attributed to the uncertainty in the empirical equation used to estimate the soil subgrade reaction, the absence of accurate measurements for soil properties and the presence of microcracks and local deteriorations that the FE model cannot tackle. Moreover, looking at the power spectrum for the different components of the noise measurements in Figs. 8 and 10, the estimated natural period ranges between 2.0 and 2.2 Hz, close to the FE model of 2.29 Hz. The numerical model of the minaret in SAP2000 is shown in Fig. 11. The results indicate that employing a soil subgrade reaction of $K_s = 11.71$ N/mm^{3}produces a fundamental period close to the ambient vibration. Therefore, all further analyses were investigated considering soil subgrade reaction of $K_s = 11.71$ N/mm^3.

The normalized horizontal displacement extracted from the ambient vibration and the FE model's modal analysis along the minaret height is plotted in Fig. 12. The ambient vibration analysis's normalized displacement represents the minaret's different sensor locations' peak displacements, particularly sensors U1, U3, and U4. Moreover, the modal analysis's normalized displacement stands for the lateral displacement x-direction of Mode 1 and y-direction of Mode 2. Since the governing

Table 1 Modal analysis results of the measured ambient vibration and finite element model with soil subgrade reaction and fixed base conditions

Mode	Frequency (Hz)			Mode description
	Ambient vibration	FFE with fixed base	FE with soil modulus subgrade reaction	
1	2.00	5.59	2.29	(x direction)
2	2.28	5.72	2.42	(y direction)
3	–	–	2.80	(z direction)
4	15.61	21.69	16.87	(x direction)
5	16.78	40.07	17.11	(y direction)

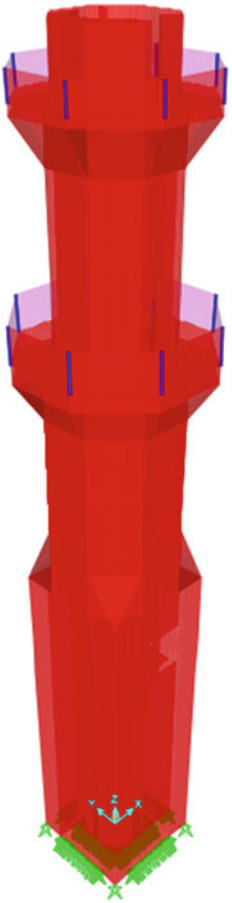

Fig. 11 Detailed finite element model of the minaret. Red colour represents the solid and shell elements, blue colour represents frame elements, and green colour represents the soil springs

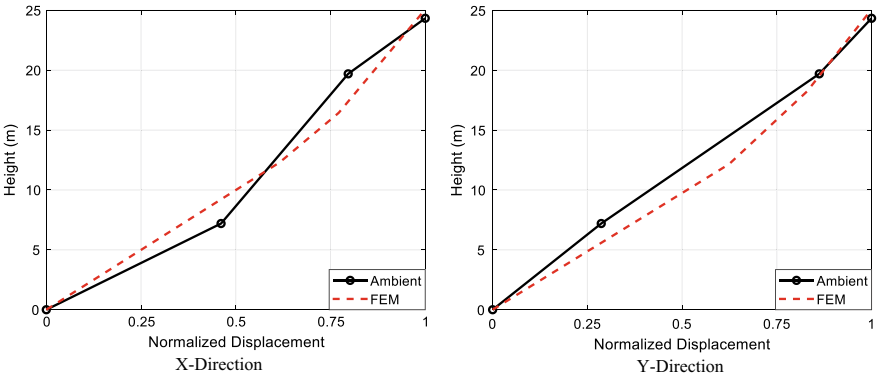

Fig. 12 The normalized horizontal displacement of the FE model modal analysis and the ambient vibration measurement points in X-Direction (mode 1) and Y-Direction (mode 2). The sensors' locations are denoted with circles

mode description of Mode 1 is the motion in the x-direction, while Mode 2 is in the y-direction. Good agreement between the normalized displacement of the FE model and ambient measurements is observed at the measurement points. Relatively less agreement took place at transition zones above the baseand the balcony slabs due to lack of measurements at these points due to the ismpracticality of installing sensors at these locations without damaging the minaret's body.

Moreover, the FE model results gave a reasonably good estimate of the minaret lateral deformation. It adapts the precise geometry, sections, openings, and stiffness variation along with the minaret height, while the ambient vibration plot represents the linear piecewise connection between the limited available three measurement points. Also, the disagreement between the results may be attributed to the numerical model deficiency in simulating the minor deterioration in the actual limestone bricks or fill material. Discarding the staircase modelling has a negligible effect on the minaret global response (Sezen et al. 2008). The previous results exhibit the field measurements' significance for such structures on tuning and evaluating the FE model's response. The FE model's tuning represents the model's mesh sensitivity analysis to determine the model's fine discretization to produce its dynamic characteristics.

The limestone selected for the numerical model has a compressive and tensile strength of -27.47 and 5.40 MPa, respectively, as previously mentioned. The principal positive (tensile) and negative (compressive) stresses are investigated, noting that the principal stresses are oriented by definition so that the associated shearing stress is zero. Using the principal stresses as a failure criterion is allowed and restricted to brittle materials, such as limestone. The peak principal stresses analysis due to the gravity loading cases is illustrated in Fig. 13. The results show that the peak principal compressive stresses are -1.02 MPa, and the peak tensile stresses are 0.23 MPa, for the three orthogonal principal stress tensor σ_{11}, σ_{22}, andσ_{33}. In detail, the peak principal compressive and tensile stresses are -0.21, -0.21, -1.02, and 0.23, 0.18,

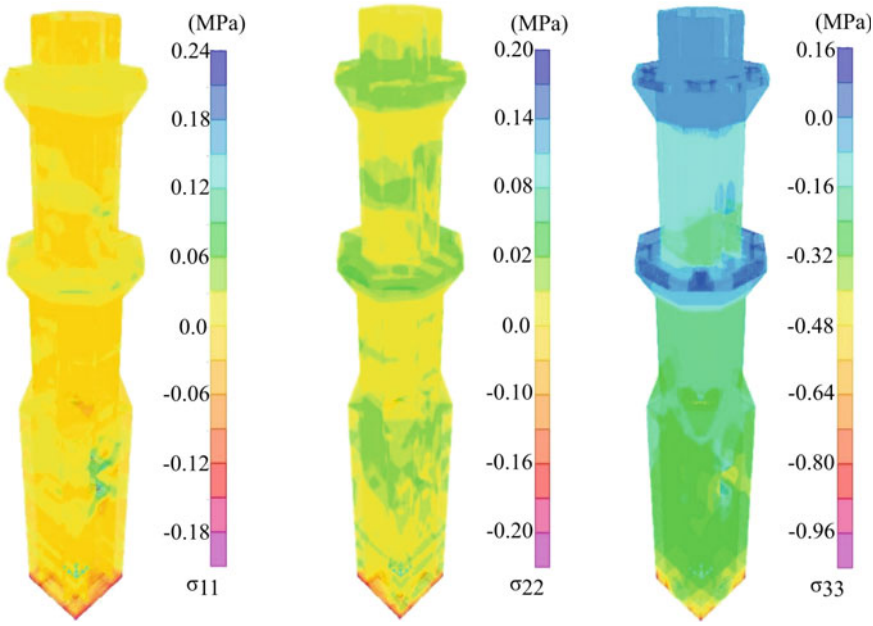

Fig. 13 Principal stresses on the minaret body due to gravity loading

0.13 MPa for stress σ_{11}, σ_{22}, and σ_{33}, respectively. The principal stresses are acceptable within the minaret construction's material stress limits defined by Imam (2001), and they indicate that the minaret can withstand its weight with no cracking.

4.3 Earthquake Response Spectrum Analysis

In this section, the linear dynamic response spectrum analysis is conducted to draw the minaret body's maximum stresses, considering the gravity load due to the minaret's self-weight. Two response spectrum analysis cases are investigated: the 1992 Cairo earthquake and the C-MCSI response spectra.

4.3.1 1992 Cairo Earthquake Spectrum

The 1992 Cairo earthquake case is selected to determine the numerical model's accuracy in detecting the minaret response since the minaret survived the Cairo earthquake in reality, with neither damage nor cracks observed after the earthquake shaking. Moreover, the 1992 Cairo earthquake's acceleration response spectrum obtained from the MCSI analysis is investigated since there are no known ground motion records for the event. Therefore, the 50th percentile response spectrum of

the 1992 Cairo earthquake is used to conduct the response spectrum analysis for the minaret model in a bidirectional horizontal direction. The principal stress results are plotted in Fig. 14. The colour limit was set to the allowable stress range, and thedark blue colour represents regions exceeding the allowable tensile stress. The results show that the peak compressive stresses are always under the allowable compressive strength with peak values of -0.21, -0.21, -1.00 MPa for σ_{11}, σ_{22}, andσ_{33}, respectively. On the other hand, the tensile stresses are high, but not enough to exceed the tensile strength, as the peak recorded principle tensile stress tensor was $2.1(0.38\sigma_t)$, $1.3(0.24\sigma_t)$, $5.1(0.94\sigma_t)$ MPa in the minaret body for σ_{11}, σ_{22}, and σ_{33}, respectively, of the material tensile strength (σ_t). As expected, the numerical model introduced an acceptable behaviour of the minaret under the Cairo earthquake response spectrum through producing undamaging peak tensile and compressive stresses within the minaret, especially at the transition zone or near the openings.

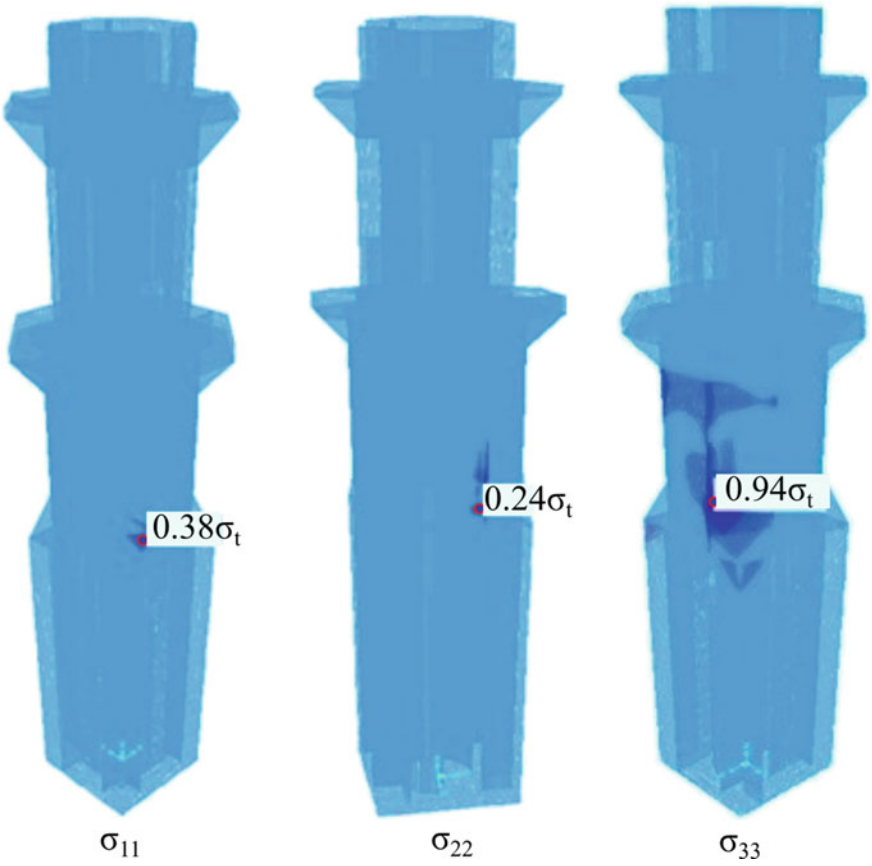

Fig. 14 Peak tensile principal stresses as a factor of the material tensile strength ($\boldsymbol{\sigma_t}$) on the minaret body under the 1992 Cairo earthquake response spectrum

4.3.2 C-MCSI Spectrum

The calculated C-MCSI at the 50th percentile spectrum is applied at the minaret base in both horizontal directions. The principal stress results are depicted in Fig. 15, and they show that the minaret would suffer significant tensile stresses exceeding the limestone tensile strength, which denotes enormous cracking and even crushing in the minaret, particularly at the base and at the transition zone right above the base. The peak tensile and compressive stresses are $4.6(0.85\sigma_t)$, $4.9(0.91\sigma_t)$, $8.9(1.64\sigma_t)$ MPa and -0.20, -0.19, and -0.93 MPa. This level of tensile stresses predicts severe damage or even the minaret's collapse under the C-MCSI response spectrum. The previous results demonstrated that the tensile stress concentrations took place at the end of the transition zone between the square base and the hexagon shaft, where the reduction of the minaret cross-sectional area occurs.

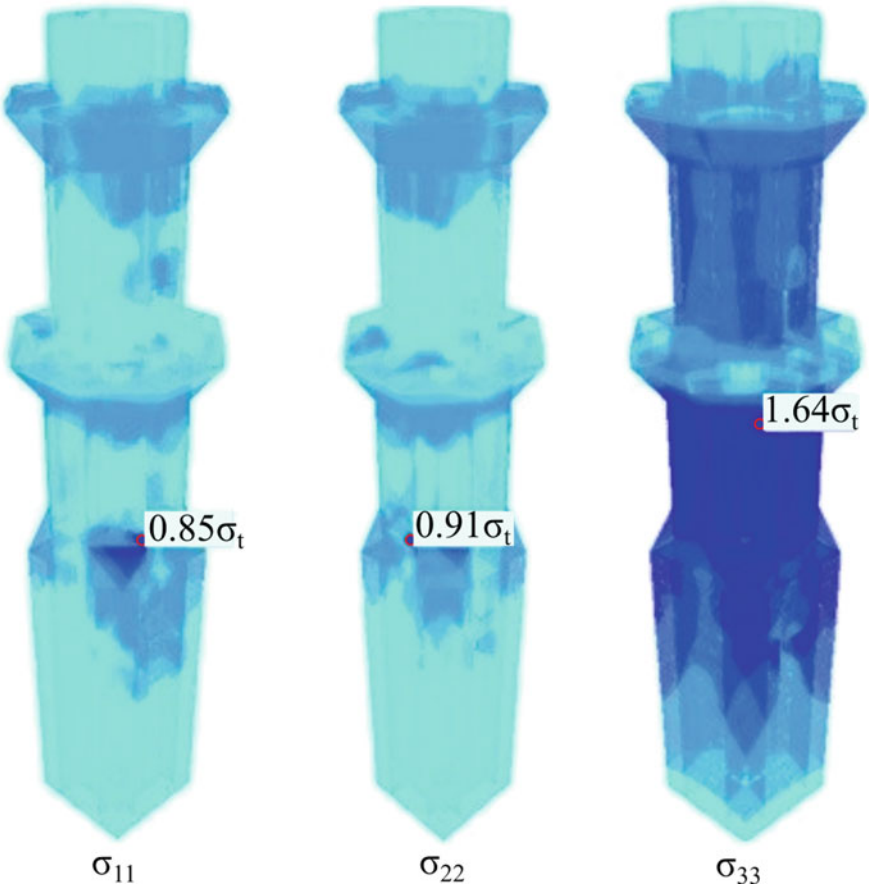

Fig. 15 Peak tensile principal stresses as a factor of the material tensile strength (σ_t) on the minaret body under the C-MCSI response spectrum

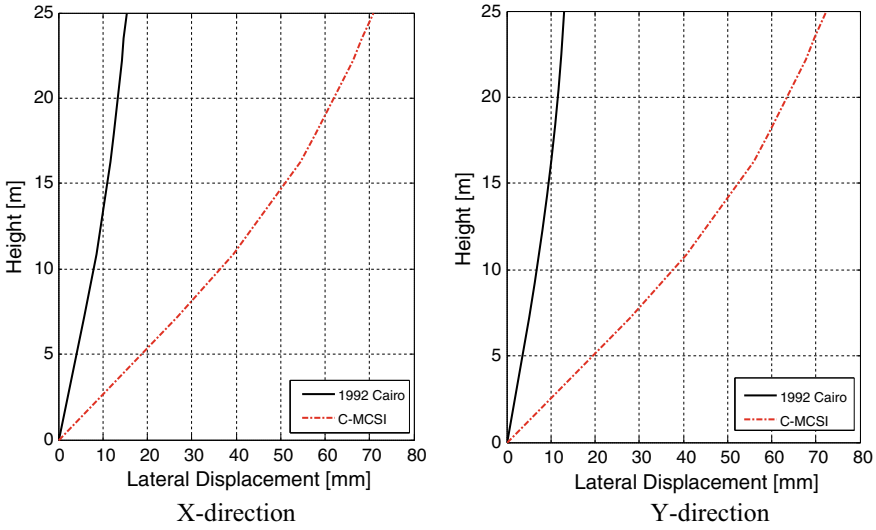

Fig. 16 Maximum horizontal displacement in X-direction (left panel) and Y-direction (right panel) under the 1992 Cairo and C-MCSI response spectra

The peak horizontal displacement along the minaret height in both horizontal directions under the 1992 Cairo and C-MCSI response spectra action is illustrated in Fig. 16. The results show that the C-MCSI analysis case developed higher lateral displacement than the 1992 Cairo case in both directions. Furthermore, the peak lateral displacement under the C-MCSI spectrum is about 70.8 and 72.8 mm in x and y-direction, respectively, compared with 15.3 and 13.0 mm under the 1992 Cairo response spectrum in x and y-direction.

4.4 Time History Analysis

The seven pairs of acceleration time histories selected in Sect. 5 are considered for conducting the minaret's dynamic time history analysis. The peak lateral displacement at the transition zone above the base and the top of the minaret in x- and y-directions are illustrated in Table 2; their fluctuation between the two orthogonal directions is mainly due to the difference between the ground motions components (NS or EW) assigned for each direction. However, it is worth mentioning that a slight difference exists in the peak displacement between the x- and y-direction due to the geometry irregularity (i.e., openings, imperfect symmetry, etc.) as seen in the C-MCSI response spectrum results in Table 2, although an identical response spectrum is applied in the x and y-direction at the minaret base.

The floor response spectra for 5% damping have been computed at the top of the minaret using time history analysis as shown in Fig. 17, where the mean of the

Table 2 Maximum horizontal displacement at the transition zone and top of the minaret subject to time history analysis

Measured point	Maximum horizontal displacement [mm]			
	Top		Transition zone	
Direction	X-dir	Y-dir	X-dir	Y-dir
Seven ground motion pairs	51.41	39.80	31.57	24.76
	63.49	54.65	39.04	33.93
	59.72	54.91	36.82	34.31
	60.20	44.37	37.17	27.75
	64.10	49.53	39.46	30.85
	59.07	31.14	36.35	19.38
	57.51	52.00	35.47	32.39
Mean	59.36	46.63	36.55	29.05
C-MCSI RS	70.80	72.80	43.70	45.20

seven response spectra is also depicted for both orthogonal directions. The spectral acceleration at the top of the minaret (base of the mabkhara or cap) is also investigated. The minaret's top describes a specific shape of the minaret finial, and it is always considered the weakest part of the minaret, i.e., more likely to collapse during ground shaking. The minaret cap (currently are not in place) already experienced damage and complete failure earlier, as noticed comparing Fig. 1b and c (Mayer and Speiser 2007). Thus, the time history analysis could be needed in the future restoration and put in place of the mabkhara. Substantial amplification occurs in the response spectra with peak ground acceleration (PGA) of 1.37 and 1.28 g, in x- and y-direction, respectively. While the input motions have an average response spectrum with a PGA of 0.4 g, as shown previously in Fig. 5.

5 Conclusions

Four earthquake scenarios consisting of one recent and two historical earthquakes are adopted to model the ground motion and compute the minaret site's seismic input using the NDSHA approach. The 1992 and 950 scenarios were used as seismic sources to model NS cross-sections under the minaret, while the 857 earthquake scenario was used as the earthquake scenario for the modelling of the EW cross-section.

We selected the seismic input (response spectra and time histories) from the database computed for the historical Cairo by Hassan et al. (2020) for the evaluation of the dynamic performance of the minaret of the Madrasa the Princess Tatar al-Higaziya, which will help in proposing a seismic conservation strategy for this valuable structure. We provide the MCSI and C-MCSI acceleration response spectra

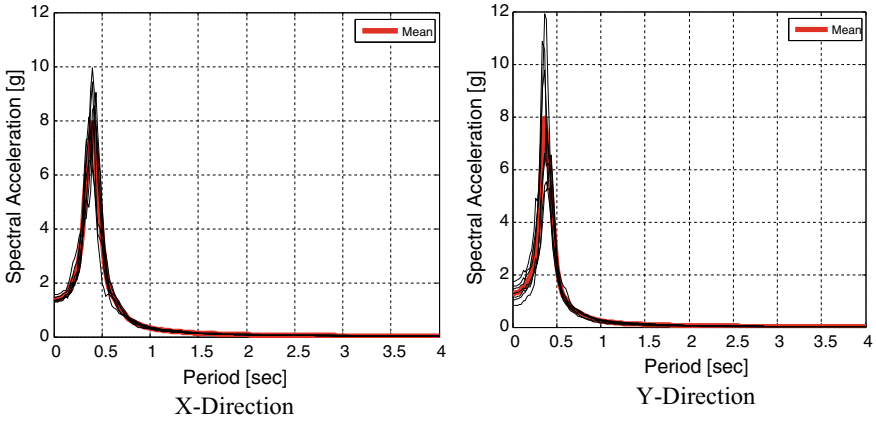

Fig. 17 Acceleration response spectra at the top of the minaret for 5% damping, in X-direction (left panel) and Y-direction (right panel)

at the minaret site to assess the minaret's dynamic behaviour by joining both seismological and engineering knowledge to understand the performance of this monument under earthquake action. The results could help recommend improved mitigation measures for the minaret while also representing a step towards the risk reduction and management of this historic structure.

A detailed numerical model for the minaret was established, accompanied by seismic sensors and ambient vibrations to evaluate the numerical model. A careful visual inspection was performed to summarize the minaret body's construction materials and elements and investigate the minaret cracking status. Two seismic analysis types were conducted for the minaret numerical model, namely the response spectrum analysis and the time history analysis. The response spectrum analysis was selected to replicate the 1992 Cairo earthquake excitation scenario since no earthquake records were preserved near the minaret's site. The numerical model adequately captured the minaret response without indicating any signs of cracking or damage, which matches the minaret's actual behaviour during the 1992 earthquake. Furthermore, the response spectrum analysis was also applied for the proposed C-MCSI$_{SS}$ spectrum; the computed C-MCSI$_{SS}$ response spectrum and time history analyses predict severe damage to the minaret. The analysis under the C-MCSISS predicts significant lateral displacements at the top of the minaret and excessive tensile stress concentration, particularly at the geometric transition zone between the squared base and the hexagon shaft.

Itis worth mentioning that the small vertical separation gap between the minaret and the wall of the Madrasa may pose a pounding potential between the adjoining structures due to the minaret's horizontal vibration. This threat will be covered in the future work of the Madrasa.

Finally, since the minaret is expected to suffer severe damage against the anticipated earthquake shaking scenario, a vital protection plan is recommended to avoid

any future damage or collapse to the structure. Stitching the walls with pre-stressed rebar or reinforcement of the walls' inner side with incorporated steel are pervasive ways for retrofitting and protecting historical monuments and structures. Besides, skins of reinforced concrete coating or fibre-reinforced plastic (FRP) on the walls' outer side may enhance the walls' tensile strength, hence improving the minaret's performance against the anticipated intense earthquake scenario.

Acknowledgements This work was partially supported by the Egyptian Ministry of Higher Education (Cultural Affairs and Missions Sector, Cairo) and by the (MAE-MHE) bilateral Egyptian-Italian project "Advanced seismic hazard assessment in the Nile Delta, including the site effects from distant earthquakes." under the Science and Technology Development Fund (STDF), Egypt, Grant No 25991 and 25553. Also, we would like to thank NRIAG for providing the noise sensors and the field logistics. Special thanks to the Ministry of Antiquities for facilitating the work and their fruitful cooperation. The authors are debited to Prof. Abbas M. Abbas, Franco Vaccari, and Dr. Nagy Naguib for their valuable contribution. The first author wants to express his thanks and appreciation for Prof. Giuliano Panza for the continuing support and inspiration.

References

Baker JW (2011) Conditional mean spectrum: tool for ground motion selection. J Struct Eng 137:322–331

Baker JW, Cornell AC (2006) Spectral shape, epsilon and record selection. Earthquake Eng Struct Dynam 35:1077–1095. https://doi.org/10.1002/eqe.571

ECP-201 (2011) Egyptian Code of Practice No. 201 for calculating loads and forces in structural work and masonry. National Research Center for Housing and Building, Ministry Housing, Utilities and Urban Planning, Cairo

El-Attar AG, Saleh AM, Zaghw AH (2005) Conservation of a slender historical Mamluk-style minaret by passive control techniques. Struct Control Health Monit 12(2):157–177

ElGabry M, Hassan HM (2021) Updated seismic input for next generation of the Egyptian building code. In: Sustainable issues in infrastructure engineering. Springer, Cham, pp 55–79

Fasan M (2017) Advanced seismological and engineering analysis for structural seismic design. PhD thesis, Trieste University, Italy

Gaber H, El-Hadidy M, Badawy A (2018) Up-to-date probabilistic earthquake hazard maps for Egypt. Pure Appl Geophys 1–28

Gorshkov AI, Hassan HM, Novikova OV (2019) Seismogenic nodes (M≥5.0) in Northeast Egypt and implications for seismic hazard assessment. Pure Appl Geophys 176(2):593–610

Hassan HM, Panza GF, Romanelli F, ElGabry MN (2017a) Insight on seismic hazard studies for Egypt. Eng Geol 220:99–109

Hassan HM, Romanelli F, Panza GF, ElGabry MN, Magrin A (2017b) Update and sensitivity analysis of the neo-deterministic seismic hazard assessment for Egypt. Eng Geol 218:77–89

Hassan HM, Fasan M, Sayed MA, Romanelli F, ElGabry MN, Vaccari F, Hamed A (2020) Site-specific ground motion modeling for a historical Cairo site as a step towards computation of seismic input at cultural heritage sites. Eng Geol 268:105524

Imam HF (2001) Technical study on the structural condition of the Tatar al-Higaziya Madrasa and minaret (monument#36). Historic Cairo Project, Stage 3, Group 3. Cairo, Egypt

Mayer W, Speiser V (2007) A future for the past: restorations in Islamic Cairo; 1973–2004. German Archaeological Institute, Cairo

Rinaldin G, Fasan M, Noé S, Amadio C (2019) The influence of earthquake vertical component on the seismicresponse of masonry structures. Eng Struct 185:184–193

Sawires R, Peláez JA, Fat-Helbary RE, Ibrahim HA (2016) Updated probabilistic seismic-hazard values for Egypt. Bull Seismol Soc Am 106(4):1788–1801

Sayed MA, Go S, Cho SG, Kim D (2015) Seismic responses of base-isolated nuclear power plant considering spatially varying ground motions. Struct Eng Mech 54(1):169–188. https://doi.org/10.12989/sem.2015.54.1.169

Sezen H, Acar R, Dogangun A, Livaoglu R (2008) Dynamic analysis and seismic performance of reinforced concrete minarets. Eng Struct 30(8):2253–2264

Sykora D, Look D, Croci G, Karaesmen E (1993) Reconnaissance report of damage to historic monuments in Cairo, Egypt following the October 12, 1992 Dahshur earthquake. Army Engineering Waterways Experiment Station Vicksburg MS Geotechnical Lab

Toni M (2012) Site response ad seismic hazard assessment for the southern part of Cairo city, Egypt. Unpublished PhD thesis, Faculty of Science, Assiut University, p 151

Vesic AB (1961) Beams on elastic subgrade and Winkler's hypothesis. In: Proc. 5 th. Int. Conf. on Soil Mech. Found. Engrg. Paris, pp 845–50

Williams C (2008) Islamic monuments in Cairo: the practical guide. American Univ in Cairo Press